Summary

This project aims to optimize the shift fork by reducing the weight of the shift fork while maintaining within the operational constraints, such as altering the shape of the shift fork such that stress exerted on the component is less than the yield stress of the chosen material and having deflection below 0.3mm.

The initial design geometries were generated through ABAQUS GUI based on dimensions shown in figure 21 from the appendix. Then linear analysis was performed, then another non-linear analysis was commenced on the same initial design. Both analysis results showed that the initial design was too conservative, as they were nowhere near the design limits only reaching a maximum stress of 10MPa in the non-linear analysis, indicating space for improvement. Initial design uses the material choice of low carbon steel which had a weight of 1.28E-3 tons and a volume of 1.65E5 mm^3.

An iterative approach was taken to optimize the weight of the shift fork, this methodology mainly consists of identifying areas of low stress distributions and removing the mass from these areas, as they wouldn't affect the component's structural integrity to dissipate stress. The final design was able to achieve a 70% weight reduction compared to the initial design as well as a 69% volume reduction, all while the simulation results stayed within the aforementioned operational limits. Mesh convergence was done, and it was decided that a locally refined mesh density has the highest accuracy to CPU time ratio. A few other materials were taken into consideration, 7068 Aluminum Alloy was selected to be the most suitable candidate due to its heigh yield strength to density ratio and it is the cheapest material which is beneficial for manufacturing.

Potential dangerous natural frequencies were obtained via linear dynamic analysis on the shift fork. The most concerning natural frequency was 1256 Hz from the 1st vibration mode. However, it was soon realized that it is still a lot higher than the natural frequency of an automobile driveshaft (the closest car component to shift fork) and the ride frequency inside an F1 racing car, thus eliminating the threats of resonance within a vehicle. Theoretical calculations for both stress and natural frequencies validated the reliability of the simulation result accuracies, both calculations presented results similar to the Abaqus simulations even with model simplifications in the theoretical calculations.

Contents

Introduction:

The power generated by the engine flows through a transmission system before it reaches the drive wheel. The transmission typically consists of gears, shafts, bearing parts and so on, and its basic function is to control the speed or torque available to the drive wheel under different driving conditions. [1] The transmission shift mechanism strength and dynamic behavior is crucial as it influences the security as well as stability of the gear shifting operations as shown in figure 1 below. Relatively, the shift fork of the transmission system is equally important (figure 2). This horseshoe shaped metal lever's main function is to facilitate the engagement of gears by shifting along the transmission axis, which then helps realize variable speeds and torques of the vehicle. Nonetheless, being exposed to constant gear pushing means that it must be designed to withstand loading on a regular basis without undergoing deformation or failing. Different vehicle use cases require different optimization approaches, e.g. for an off-road vehicle, a shift fork with a longer life span and a stronger material would be preferred. Whereas in F1 racing, a shift fork's weight would be considered more important.

Figure 1: The Structure of lorry's shift mechanism [1]

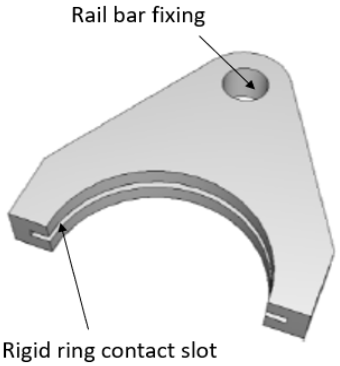

Figure 2: Diagram of the shift fork component

Objective:

The goal of this project is to utilize ABAQUS (a commercial Finite Element Analysis (FEA) program) to perform stress and strain analysis on the shift fork component and use these results to reduce the mass of the shift fork component, all while exhibiting responses that are within the design criteria stated below. The fork's axil movement function, manufacturability and cost should also be considered.

Design criteria:

The main dimensional modification restrictions are listed in the assignment briefing in figure 14 from the appendix, where the dimensions are detailed in a red box. Further simulation requirements are:

- **The maximum stress** simulated of the fork may not exceed the yield strength of the chosen material
- **The maximum deflection** (deflection in the U3 direction in the model) simulated may not exceed 0.3mm.

The load applied in all simulations are calculated via the student ID:

$$1915 - 700 = 1215\,N \qquad (1)$$

Initial design linear analysis:

The initial design dimensions for the shift fork components is given in figure 14 from the appendix.

Quantity	Length	Force	Mass	Time	Stress	Energy	Density
SI unit	mm	N	ton (10^3 kg)	s	MPa (N/mm^2)	mJ (10^{-3} J)	ton/mm^3

Table 1: SI units used in all simulations

Material	Low Carbon Steel
Young Modulus (E)	210 GPa
Poisson ratio (v)	0.3
Mass density (ton/mm^3)	7.8 E-9
Yield Strength	220 MPa

Table 2: Initial material properties

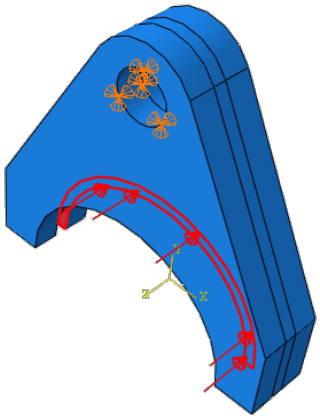

Figure 3: The Boundary condition and load applied in the linear analysis of the initial design

In the initial design, material properties indicated in table 2 is applied into the material property section. The SI unit system utilized in this report is shown in table 1. The initial design's geometry is generated in Abaqus CAE's GUI. The overall mass of the initial design is 0.00128 ton which is relatively heavy. As mentioned, a linear analysis is performed on the initial design of the shift fork component, firstly a boundary condition is applied to mimic the fixed rail connection surface through the top of the hole, demonstrated in figure 3, where the displacements degrees of freedom are restricted and that the deformed body will not have rotation. Afterwards, a fixed pressure loading of 2.102MPa is applied to the surface also indicated in figure 3 as the red arrows. This is calculated by probing the contact surface area was probed to be 578.1 mm^2. (Unique fork axial load calculated in equation (1), then using $Pressure = \frac{Force}{Area}$ to calculate the input pressure load for the model)

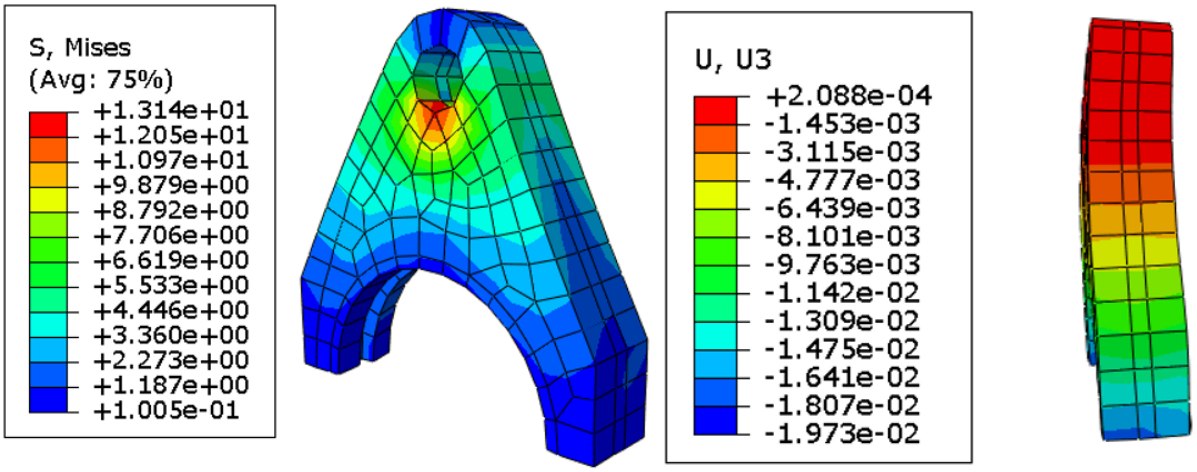

Figure 4: Von Mises Stress in the linear analysis

Figure 5: Deflection (U3 direction – axial) in the linear analysis

Linear analysis results

- It is worth noting that the total number of elements utilized in this linear model is 261 with the linear hexahedral element type of C3D8R and the plots are applied with a deformation scale factor of 608, for more obvious visualization of the deformation.
- Figure 4 shows the **maximum von mises stress** of 13.14 MPa near the fixed rail connection hole on the shift fork component but it is only around 6% of the aforementioned yielding point (220MPa). Other than the peak stress, stress is distributed uniformly throughout the shift fork.
- The **maximum deflection** was indicated to be 0.01973 mm, 6.57% of the maximum allowable deflection, displayed in figure 5 with a deformation scale factor of 608.

This indicates the current initial design not only has no problem meeting the minimum criteria's but actually too conservative, there is potential to decrease the weight of the whole shift fork component by changing its geometry, more specifically volume reduction. Moreover, different materials could be used to decrease weight while possessing high enough yield-strength to withstand the stress experienced during the shifting of gears.

Initial design non-linear analysis:

The Abaqus CAE non-linear solver utilizes the Newton's Raphson's method to generate solutions (An iterative method of approximating the solution of an equation $f(x) = 0$ where the process is repeated until a solution converges). The non-linear model consists of creating a rigid ring, done by adding a reference center point on the plate, boundary condition is then added to the reference point to restrict all degrees of freedom except the one in the direction of the loading (U3 in this case), it is worth mentioning that the fixed rail boundary condition is still applied in this case. In this model, a concentrated point load of -1215N is applied to the center of the ring in axial direction (CF3 direction) as shown in figure 6. All nonlinear analysis is shown with a **deformation scale factor** of 608 for better visualization.

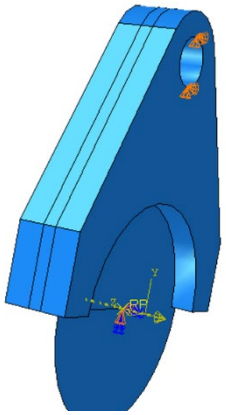

Figure 6: Non-linear model of the shift fork

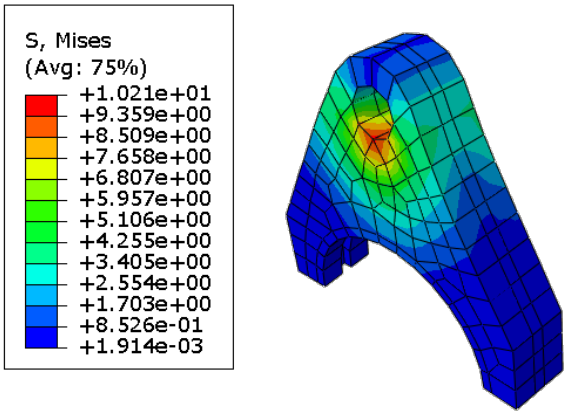

Figure 7: Von Mises Stress in the non-linear analysis

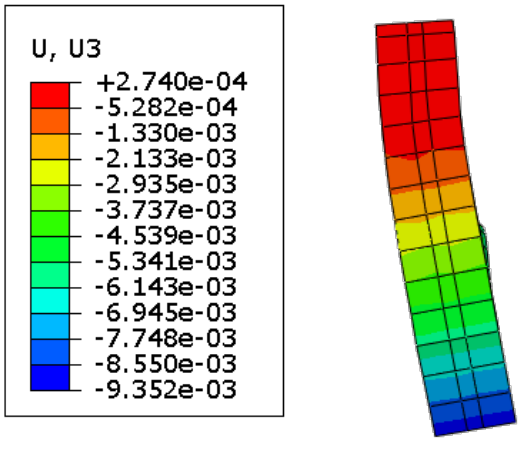

Figure 8: Deflection (U3 direction – axial) in the non-linear analysis

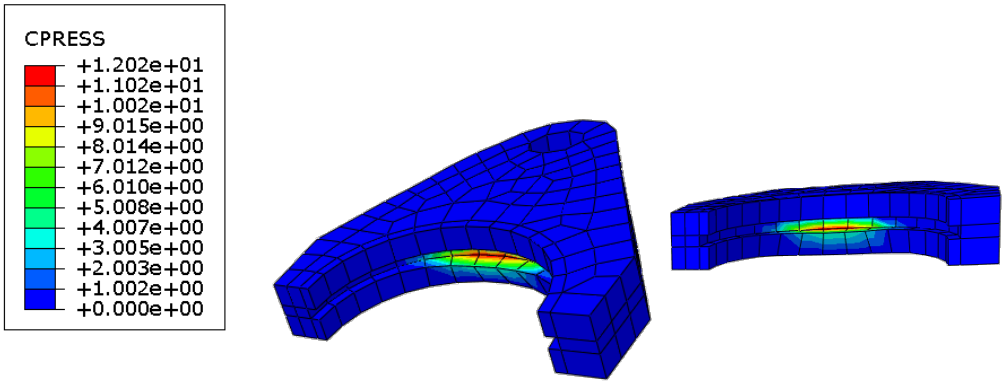

Figure 9: Contact Pressure of the initial design in the non-linear analysis

- The nonlinear analysis result on the initial design shows a **maximum stress** of 10.02 MPa (figure 7) which is similar to the linear analysis (13.14 MPa). Stress distribution remained the same, concentrated near the region of the fixed railing.
- **Maximum deflection** was 0.00932 mm (figure 8), also similar to the linear analysis. Both are still within the requirements as expected.

One can identify local contact pressure (CPRES) in the non-linear model, where the pressure between the contacts is concentrated, reflecting the behavior of the shift fork component, which was not displayed on the linear model, as demonstrated in figure 9. Although maximum pressure experienced in the non-linear analysis is a lot higher than the linear analysis, one can see through figure 9 that the pressure region is a lot smaller compared to the linear analysis where pressure acted along the slot in figure 3. This means that overall force the shift fork experience in the non-linear analysis is a lot smaller, explaining the smaller overall stress and deflection exhibited in the non-linear analysis results in figure 7 and figure 8. It is worth noting that there is also a different in stress distribution near the contact slot between the rigid ring and the shift fork. In the linear analysis, stress is more uniformly distributed throughout the slot, whereas in the non-linear analysis, the stress is a lot more localized near the center of the slot.

Design improvement:

An iterative approach is taken to gradually improve the geometry design of the shift fork component. Each iteration utilizes the results of the non-linear analysis to identify areas of low stress and allows for volume reduction, without affecting the performance of the shift fork components.

Iteration 1:

Development:

From figure 7 and figure 8, one can see that stress is not concentrated near the middle of the bottom. Therefore, a rectangular slot was extruded through the whole shift fork in the axial direction, as that area is stress free. It is worth noting that everything else such as boundary conditions, contact interactions and load magnitudes still remain the same as the non-linear model initial setup.

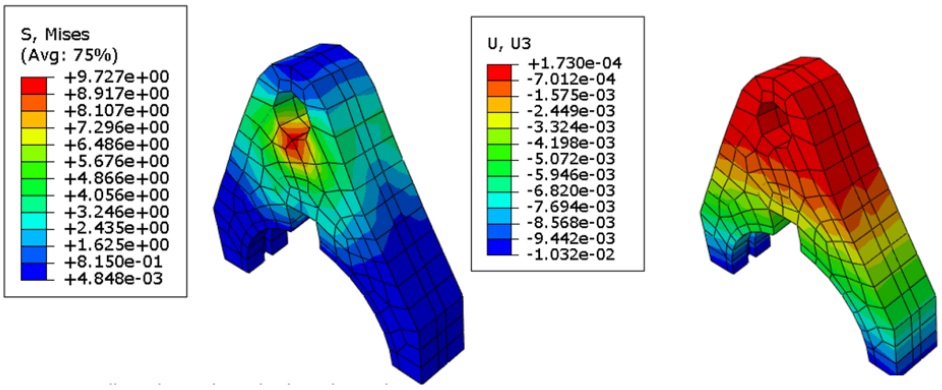

Figure 10 Stress distribution & deflection (U3 direction – axial) of the non-linear analysis on iteration 1

Results and analysis:

- The results show that a new **maximum stress** of 9.727 MPa, less than the initial design. Since only area not affected by stress is extruded, thus it is expected that maximum stress didn't change much. Nonetheless, stress is still well below 220MPa.
- **Maximum deflection** was 0.0103mm, a 0.001mm increase compared to the initial design and well within the 0.3mm deflection criteria. Since this extrusion doesn't affect the stress much, consequently the deflection won't change either from this minor shape change.
- The **mass** has decreased down to 0.00124 ton which is a bit lighter than the initial design (0.00128 ton).

Iteration 2:

Development:

In this iteration, the weight of the shift fork is further reduced by drilling two holes near the main fixed rail slot. This can help redirect some stress lines around the main hole rather than removing the outer part surrounding this region. As seen from previous iteration, the highest stress is concentrated near the main hole, displayed in figure 10.

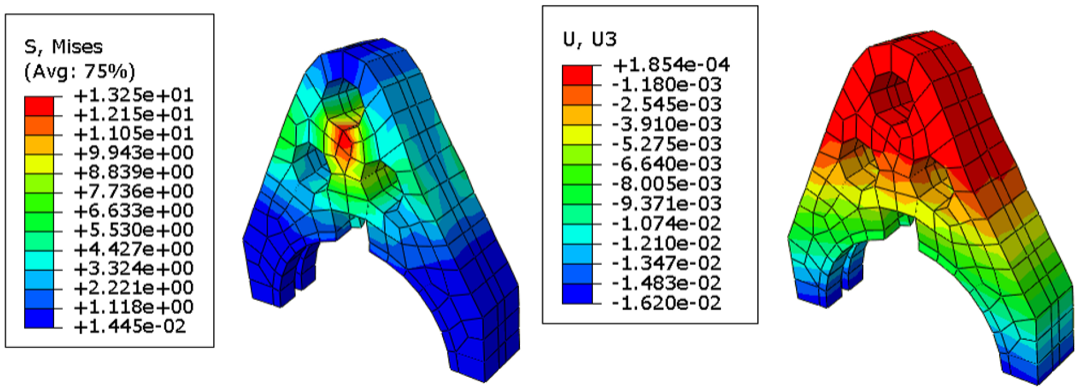

Figure 11: Stress distribution & deflection (U3 direction – axial) of the non-linear analysis on iteration 2

Results and analysis:

- The highest **stress** being 13.25 MPa, which is only a slight increase in stress experienced in iteration 1, the added holes help redirect stress lines but there's less mass so an increase in stress overall makes sense.
- **Deflection** has also increased to 0.0162mm, which may stem from slight increase in stress experienced.
- This are to be expected as the whole shift fork has decreased its **mass** to 0.00113 tons (1.13 kg), so it's bound to be easier to displace.

Iteration 3:

Development:

Since the maximum deflection is still way below 0.3mm, the Shift fork component thickness has been cut down by 10mm total (5mm of thickness reduced from both sides in the axial direction) This is the quickest way to reduce weight, as well as save material cost from manufacturing with less resources needed to manufacture a thinner shift fork. There is also no drastic geometric change so manufacturing process will still remain the same.

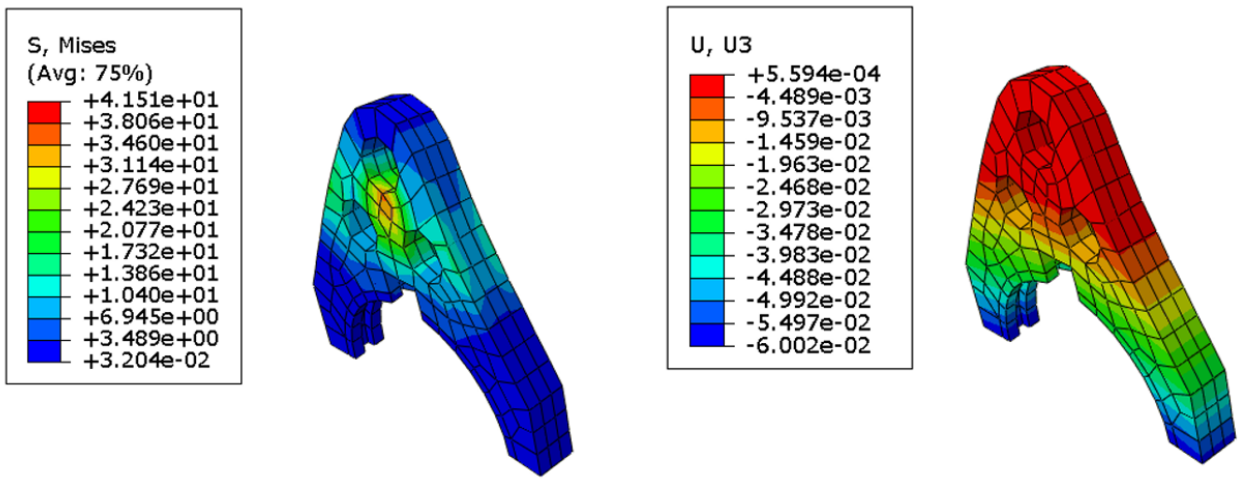

Figure 12: Stress distribution & deflection (U3 direction – axial) of the non-linear analysis on iteration 3

Results and analysis

- The **maximum von mises stress** experienced has increased considerably to 41.4 MPa (figure 12). This was anticipated due the amount of mass removed from the shift fork, meaning there is less mass to help endure the stress. The thinning was symmetric hence the stress distribution doesn't change.
- **Maximum deflection** is 3.75 times of the previous iteration which is 0.06mm. This is obvious from the increased stress experienced.
- The analysis has shown huge improvements, the **mass** decreased down to 6.72 E-4 tons (0.672 kg), which is 59% of the weight of iteration 2 as well as volume reducing to 86116 mm^3, also 59.3% of the previous iteration volume.

Iteration 4:

Development:

It was shown on figure 12 that there is very little stress distributed on the side of the shift fork. 2 Holes were drilled into the sides of the shift fork component (x-axis of the model) to reduce the weight. The holes were positioned so that it doesn't affect the smoothness of the rail movement in the axial direction nor any of the restricted dimensions. It is an easy change, as it could be done during manufacturing with using a drilling machine, thus no further equipment cost is needed. The model could not be meshed using quadrilateral elements due to the complexity of the shape after adding the side holes. Hence tetrahedral elements were utilized instead as displayed in figure 13. Also, the analysis could not be started as the initial time step was too large, so it was changed to start at 0.001 timestep with the minimum time increment size changed to 1E-10.

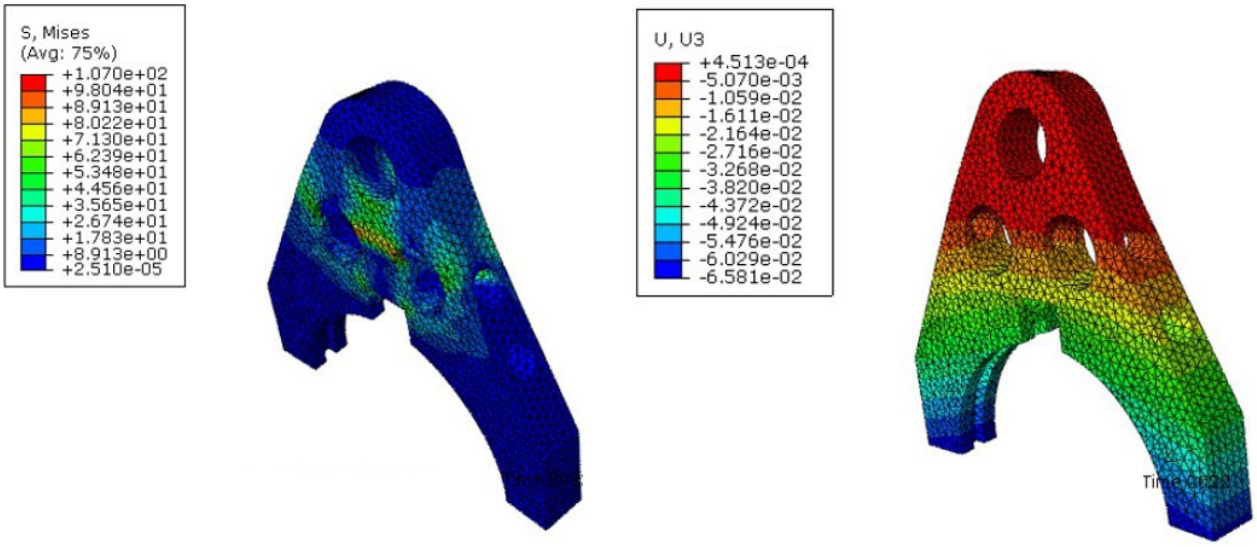

Figure 13: Stress distribution & deflection (U3 direction – axial) of the non-linear analysis on iteration 4

Results and analysis:

- Surprisingly, the stress is no longer concentrated around the fixed rail connection hole but actually the near the two holes drilled during iteration 2. The **maximum stress** in this simulation is 107 MPa (figure 13), which is double the stress of iteration 3 but still within the requirements.
- The **deflection** has increased a bit more to 0.0658mm, even when stress has doubled.
- **Mass** has decreased down to 5.905E-4 tons (0.5905 kg), which is 12% lighter than the previous iteration.

Iteration 5:

Development:

Grooves were added along the ring contact area with the shift fork, at the bottom. This is done as there is no stress distributed along the bottom of the shift fork, as shown in figure 13. Furthermore, it was proposed to remove most of the outer material near the fork sides, which were not in the concentrated stress area. Intuitively, cutting down these areas will decrease weight without affecting the overall shift

fork's ability handle the stress exerted. These changes could be completed using waterjet cutting on the low carbon steel.

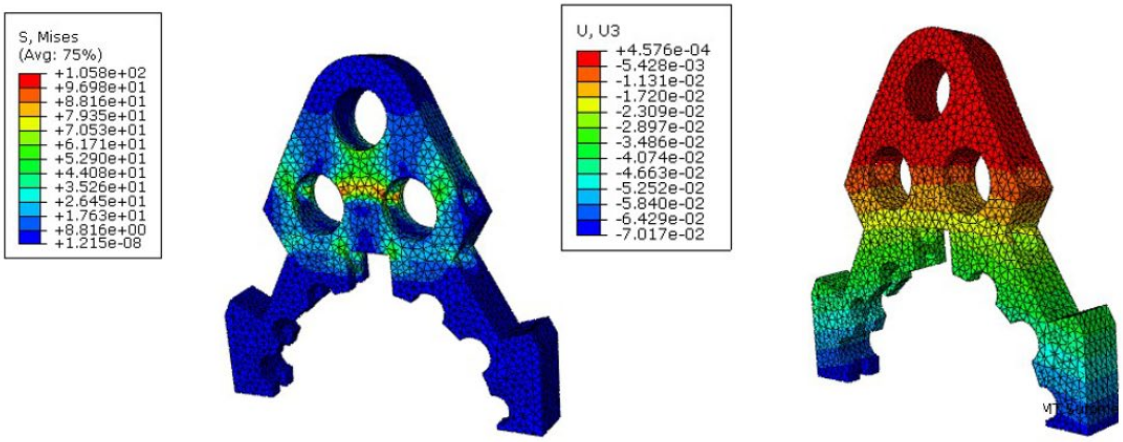

Figure 14: Stress distribution & deflection (U3 direction – axial) of the non-linear analysis on iteration 5

Results and analysis:

- **Maximum stress** experienced hasn't changed much, fluctuating around 105.8 MPa, with stress still distributing at the same spot as iteration near the 2 holes drilled under the main rail fixing hole, presented in figure 14. This is to be expected, as the mass is removed based on stress distribution of iteration 4.
- The **maximum deflection** has increased to 0.0702mm (figure 14), which was anticipated as stress didn't increase much.
- Nonetheless, **mass** has decreased down to 4.79E-4 tons (0.479kg). Volume has now decreased down to 6.14E4 mm^3, now being 71% of iteration 3's volume.

Iteration 6:

Development

The bottom corners near the ends of the fork were cut off, since there isn't much stress focused around that area. Moreover, sharp corners tend to experience high stress compared to smooth surface or fillet corners. This shape optimization has made the whole shape into a much simpler geometry at the bottom, which is advantageous for manufacturing.

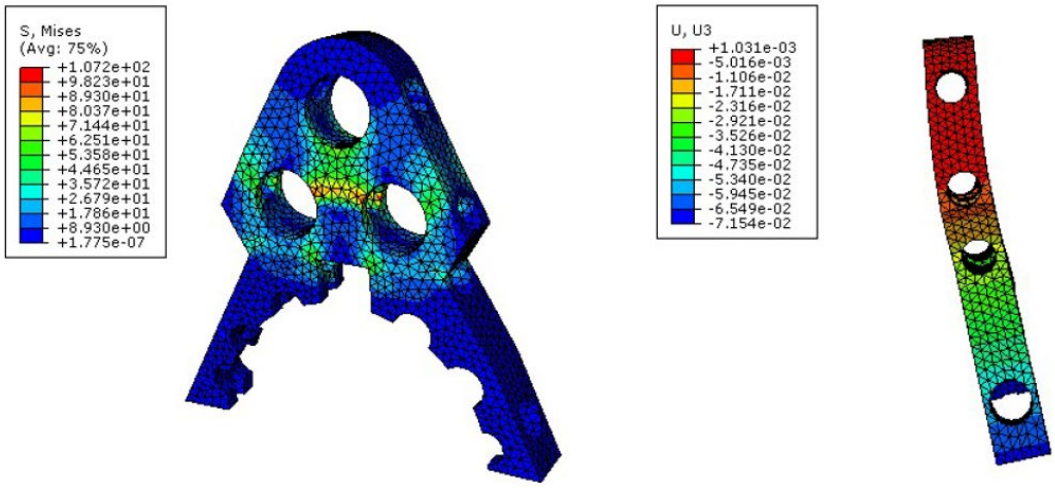

Figure 15: Stress distribution & deflection (U3 direction – axial) of the non-linear analysis on iteration 6

Results and analysis:

- The **maximum stress** again fluctuates at 107 MPa (figure 15) and stress is distributed at the same area. This shows that the corners removed were not helpful in dissipating stress before anyway thus were feasible to remove.
- **Deflection** has only increased up to 0.0715mm, a similar displacement to iteration 5.
- The shape of the displacement has altered, there is a sharp turn near the 3rd hole down from the top instead of a gradual bending in iteration 2. This makes senses as that is where the sharp corner is situated (figure 15), transitioning from the main key body to the fork at the bottom.
- Nonetheless, the **mass** continues to go down to 3.89E-4 tons (0.389 kg), another 18.8 % mass reduction. The overall volume has also decreased to 4.99E4 mm^3, a 18.7% decrease in volume. This shows consistent weight improvements from iteration 4 with minimum change in stress experienced.

Iteration 7:

Development:

Mass reduction at the center of the shift fork component was explored, where the midpoint of the shift fork is mainly hollow now. This was to test what happens when mass at the high stress area is removed but it was removed in such a curved fashion, to prevent any sharp corners producing extremely high stress.

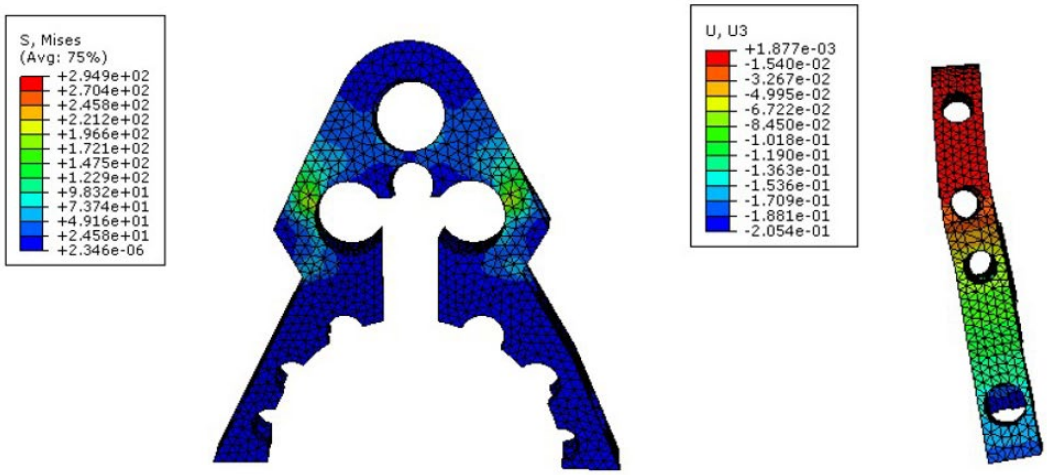

Figure 16: Stress distribution & deflection (U3 direction – axial) of the non-linear analysis on iteration 7

Results and analysis:

- The **maximum stress** in this case is 290MPa, which exceeds the yield stress of the low carbon steel. Moreover, the stress is no longer concentrated at the fixed rail slot but dispersed near the outside edges of the shift fork component, as shown in figure 16. This distribution is to be expected since there is no structure in the middle to help dissipate stress due to the mass removal, thus increasing stress throughout the rest of the component.
- **Maximum deflection** consequently increased extensively to 0.205mm, now 68% of the criteria but is still within the deflection limit. Shape of deflection remained the same as iteration 6.

- **Mass** has decreased down to 3.5E-4 tons (0.35 kg), although it is only a 10% decrease in weight, it has increased the stress doubled the maximum stress exerted on the component. Demonstrating the importance of where the mass is reduced. Volume has decreased slightly to 4.49E4 mm^3.

Iteration 8 & 9:

Development:

Due to the failure of the previous iteration. A bridge in was repaired in the center of the shift fork, more specifically, the top circular slot in between the 2 added holes was refilled (figure 22 from appendix), as that area is where most stress is concentrated, this may help re-establish structural integrity to dissipate the stress generated near that area. Another attempt in filling the gap in the center of the shift fork was commenced, by bridging the gap at the center of the bottom rigid ring slot (figure 12 from appendix). Iteration 9 again focuses on improving the center, as the center of the shift fork is crucial in helping to disperse the stress.

Results and analysis:

- ***Iteration 8:*** The refill of circular slot in the middle didn't help as the **maximum stress** was still 293 MPa (figure 22 from appendix), therefore even more support is needed in the center. The stress is still distributed along the outside of the 2 drilled holes on the face of the shift fork.
- The **highest deflection** in this case was 0.2036mm, a 0.68% deflection reduction but could be negligible due to the magnitude. The deflection pattern is unchanged from iteration 7.
- The **mass** of the shift fork has increased to 3.622E-4 tons (0.362 kg) due to the filling of the circular slot under the fixed railing hole. Accordingly, the also grew slightly to 4.644E4 mm^3.
- **Iteration 9:** The **Maximum Stress** is decreased down to 233 MPa (figure 23 from appendix), proving the effectiveness of rebuilding the middle section of the shift fork in handling the stresses.
- The **maximum deflection** in the axial direction has decreased down to 0.181mm which is well within the criteria, and the decrease is simply a product of the better dissipation of stress.
- The **mass** has further increased to 3.82E-4 tons (0.382 kg) and volume has also increased a bit to 4.898E4 mm^3, which are all results of the bridge fill at the middle of the shift fork, demonstrated in figure 23 from appendix.

Iteration 10 – Final design:

Development:

As previous 2 iterations have exceeded the constraint for maximum stress, methods of refilling the center of the shift fork where most stress are focused is further attempted all while trying to maintain lightweight. The optimal solution was established to be adding a vertical slit added in the middle of the shift fork component, providing more structural integrity, and dispersing the focus of the stress near the 2 holes underneath the main rail fixing hole.

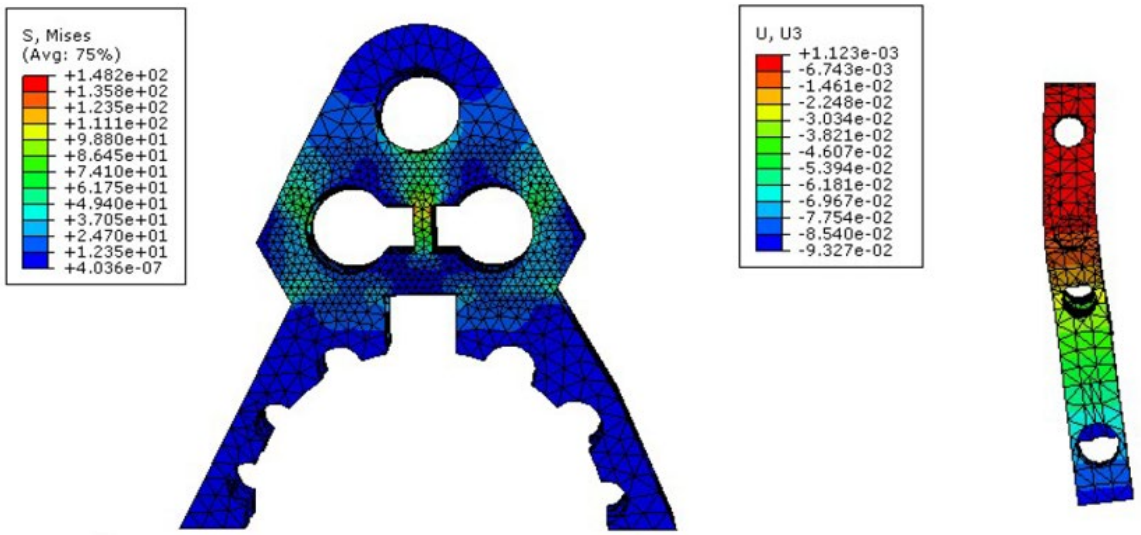

Figure 17: Stress distribution & deflection (U3 direction – axial) of the non-linear analysis on iteration 10

Results and analysis:

- As anticipated, the **maximum stress** has now distributed around the newly added slit and has decreased significantly to 148 MPa (figure 17) which is almost 63% of the iteration 9, showing the verifying the efficiency of this methodology, by increasing structural integrity through reinforcing area of high stress concentration. Moreover, the stress exerted is now within the yield strength of low carbon steel.
- Due to the stress reduction, the **maximum deflection** has also reduced to 0.0933mm, 50% of the previous iteration and is well within the acceptable operational criteria. The shape of the deflection is also smoother instead of a sharper turn observed in iteration 7.
- The contact area between the shift fork component and the rigid ring has minimized to just two spots near the middle of the contact slot, shown in figure 19 from the appendix. Therefore, with a smaller area, the maximum contact pressure has increased considerably compared to the result of the non-linear analysis on the initial design, 12 times the contact pressure of the initial design, seen in figure 9.
- The **final design's weight** has increased slightly more to 3.873E-4 tons (0.3873 kg), a 1.38% increase in weight compared to iteration 9 yet it was able to dissipate much more stress. The final volume is measured at 4.96E4 mm^3.

The part has been analyzed and optimized since there is no longer any mass on the shift fork component that is not essential for dispersing stress and removal of any of these areas will ruin the structural integrity of the overall shift fork component, ultimately exceeding yield strength of the low carbon steel.

Mesh convergence (after final design):

We consider the influence of mesh density on 2 particular results from this model:

- Maximum deflection at the bottom of the shift fork component in the axial direction
- The peak stress near the stress concentrated area at the center of the shift fork component

Locations of these 2 interests can be seen in figure 18. The stress analysis performed by ABAQUS can output more accurate results with denser mesh, this could be done by decreasing the global seed sizes,

which in turns increases the number of elements. The stress results for each of the four mesh densities (shown in figure 18) are compared in table 3, along with the CPU time required to run each simulation. It is worth noting due to complexity of the shift fork shape, tetrahedral elements were utilized in the mesh convergence, more specifically with the C3D10 element type.

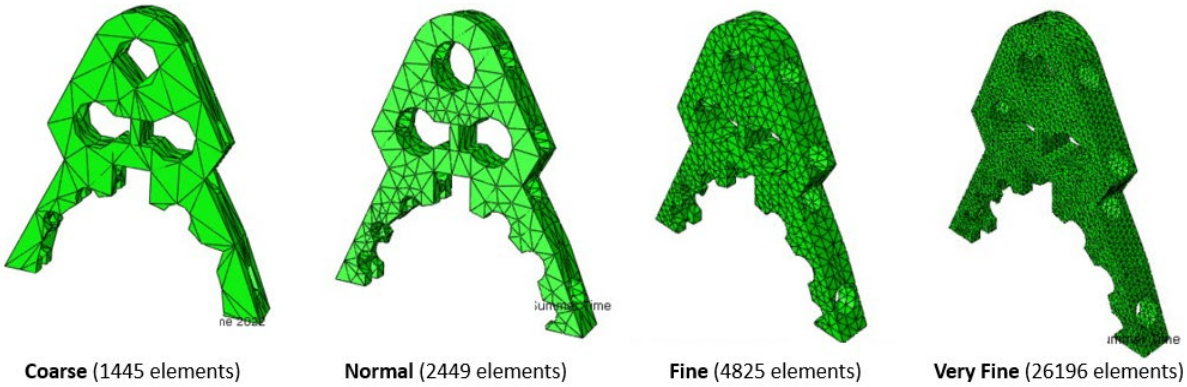

Coarse (1445 elements) **Normal** (2449 elements) **Fine** (4825 elements) **Very Fine** (26196 elements)

Figure 18: Different mesh densities with number of elements used in each category

Mesh density	No. of elements	Maximum Stress (Mpa)	Maximum Deflection (mm)	Relative CPU time (s)
Coarse	1445	94.4	0.0775	54.9
Normal	2449	114.1	0.0889	62.0
Fine	4825	124.8	0.0922	65.8
Very fine	26196	134.7	0.0927	202
Locally refined	9421	148.0	0.0933	86.3

Table 3: The simulation results of the different mesh densities

Table 3 indicates the coarse mesh predicts a less accurate maximum stress experienced and the maximum deflection on the shift fork component. Even though the normal, fine, and very fine mesh have less variation in deflection results (figure 26), the stress results don't seem to be converging. Mesh refinement significantly changes the stress calculated at the middle of the shift fork component, it continues to increase with continued mesh refinement, this can be explained by stress singularity at the corner of the middle of the slit shown in figure 17. Theoretically the stress is infinite at these sharp corners, hence increasing the mesh density will not converge the stress value at this spot (figure 25). Singularity occurs due to idealizations used in this finite element model, e.g., in this case the corners are modelled as sharp corners, but in reality, there will be a small fillet at these corners, but these are not necessary to simplify the model and can be omitted as it has a negligible effect on the overall response of the model.

Partitioning:

In practical situation, it is inefficient to use a uniformly fine mesh throughout the structure being analyzed, thus in this case a fine mesh is only used in areas of high stress gradients and a coarser mesh in areas of low stress gradients where the magnitude of stresses is not of interest in the shift fork component, figure 19 shows the mesh that is designed

Locally refined (9421 elements)

Figure 19: Locally refined mesh

to give an accurate prediction of the high stress concentrations. The result of this locally refined mesh is also stated in table 3, its results outputted are comparable to those from the very fine mesh but the simulation with the locally refined mesh requires considerably less CPU time than the analysis with the very fine mesh, 86.3 seconds, almost 3 times less than the very fine mesh simulation. Hence this is considered as the critical mesh density.

Material Consideration:

Material	Youngs Modulus (GPa)	Density (ton/mm3)	Mass (ton)	Yield Stress (Mpa)	price (GBP/KG)
Titanium Alloy	115	4.88E-09	2.42E-04	880	20.45
7068 Alumnium Alloy	73.1	3.04E-09	1.51E-04	590	2.81
CFRP epoxy matrix	110	1.71E-09	8.49E-05	255	30.9

Table 4: Material choices for the shift fork component

Material properties play a huge role in deciding the shift forks weight as well as its strength. Thus, material data was retrieved using the GRANTA Edupack material selector to assess the choice of material used in the final design (figure 27). Titanium Alloy (more specifically Ti-6Al-4V (Grade 5)) has the highest yield stress (880MPa), 4 times of low carbon steel, with a Youngs Modulus of 115 GPa. It's density of 4430 kg/m3 makes it almost half the weight of low w carbon steel. [2] Also its melting point of 1668° c allows it to work under high friction conditions. CFRP epoxy matrix provides an even lighter option by having a density of 1.71 E-9 ton/ mm^3 but its yield strength is a lot lower compared to other 2 options as well as having an extremely high material cost. Hence, 7068 Aluminum Alloy was considered the best choice, it has a high yield strength of 590 MPa, possesses a lower density than titanium and it is the cheapest. This provides a material with high strength, high ease of manufacturing with low material cost.

Linear dynamic model – obtaining natural frequency:

A Linear dynamic model was created to find the natural frequencies of the final design. The number of eigenmodes requested in this case is 10, as normally they dominate 95% of the responses. The total effective mass in the z-component of the shift fork is 1.35E-4. Dangerous frequencies were identified at modes with an effective mass in the z-component that is of the same magnitude of the total effective mass. Mode 1 and 6 were identified possessing potentially dangerous frequencies, with effective mass of 9.5E-05 and 3.2E-05 respectively.

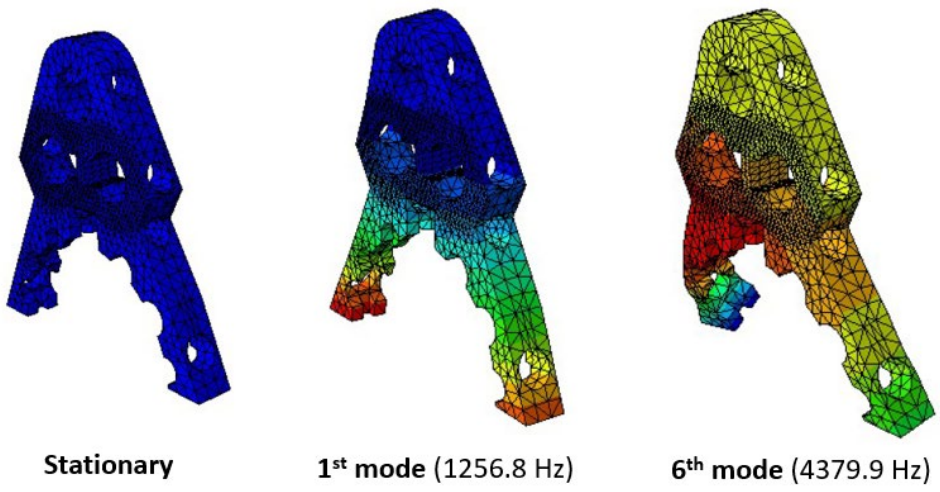

Figure 20: Various vibration modes of the shift fork component

Mode 1 & 6 has frequencies of 1256.8 & 4379.9 cycles/time respectively (figure 20). Intuitively, as the shift fork's nearest car part would be the drive shaft, their natural frequencies are compared to check for potential resonance issues. Modal analysis done by [3] shows the shaft rotating at a natural frequency of roughly 277 Hz, which is far away from the natural frequencies of both modes.

Typical ride frequencies are also considered, which is the undamped natural frequency of the body in ride. Typical ballpark numbers include 0.5-1.0 Hz on a passenger car and 2.5-3.5 Hz on Non-Aero racecars (moderate downforce Formula cars) [4]. These frequencies are still way below the 2 modes natural frequency and doesn't pose any resonance threat.

Validations: (static and dynamic analysis)

Static stress:

The stress results for the final shift fork design were compared to theoretical calculations to check its accuracy. During the theoretical calculation, the model was simplified as a simple cantilever bending of length L, width of F and thickness of t. A concentrated load W is applied at the end of the fixed beam. From the engineering data book, the equation for stress is expressed as [5]:

$\sigma = \frac{M\,C}{I} = \frac{6\,W\,L}{F\,t^2}$ where I denote the second moment of Area **(2)**

As seen in figure 17, deflection happens mostly at the bottom of the shift fork component or the end of the forks. Therefore, the second moment of area is calculated by assuming rectangular cross-sectional areas at the end of the forks. Moreover, for more accurate representation, the model consists of two bending beams.

$\sigma = \frac{6 \times 1215 \times 120mm}{60mm \times (15mm)^2} \times 2 = 129.6$ MPa

Using equation **(2)**, the theoretical stress calculated was 129.5 MPa, compared to the analysis result of 148MPa which demonstrates a 12.5% relative error, which shows acceptable results as they are the same magnitude. This error could be explained by the oversimplification of the model, as realistically the force is not directly applied at the end of the shift fork and the shift fork is not shaped as a beam. Furthermore, the calculations assume a solid fill within the shape, whereas realistically there are gaps and holes inside the shift fork. This inconsistent cross-sectional area would lower the overall second moment of area, in turn, increasing the stress induced explaining the higher value obtained during simulation.

Natural Frequency:

As for the validation of the natural frequencies obtained, the system is modelled as a simple mass-spring system, where the frequency can be expressed as:

$f = \frac{1}{2\pi}\sqrt{\frac{k}{m}}$ **(3)**

where m is the mass found from the Abaqus query tool, k is the spring constant calculated using Hooke's law from the deflection:

$k = \frac{F}{\delta} = \frac{1215}{0.0933 \times 10^{-3}} = 1.302E7\ N/m$ **(4)**

Using this spring constant retrieved, the theoretical natural frequency can be calculated as:

$f = \frac{1}{2\pi}\sqrt{\frac{1.302E7}{0.3873}}$ = 922.78 Hz

although this is not identical, it is close to the natural frequency of the 1st mode (1256.8 Hz), with a 26% relative error. This disparity could be explained by the oversimplification of the model. Nevertheless, it still validates the authenticity of Abaqus outputs, as they are of the same magnitude.

Conclusions and recommendations of further work:

Overall, the shift fork was successively optimized, with the mass being reduced from 1.28kg to 0.387 kg, which is a 70% mass reduction. Not to mention the volume has reduced from 1.65E5 to 4.96E4 mm^3, a 69% volume decrease.

The final design experienced a maximum stress of 148MPa, which is way below the yield stress of low carbon steel (220MPa). Moreover, after some material selection, 7068 Aluminum Alloy was chosen as the most suitable material for due to its high strength to weight ratio as well as having the lowest cost amongst the other materials taken into consideration. The new yield strength of the shift fork will be 590 MPa, this means that the maximum stress exerted on the shift fork has only reached 25% of the yield strength so there is no chance of material failure as tested in figure 28 from the appendix, with maximum stress of 147MPa and a new weight of 0.13kg. Therefore presenting a weight reduction of 90% with new material choice.

The deflection of the shift fork's final design is 0.0933mm for low carbon steel, remaining well under the constraint of 0.3mm. However, due to the new material selected, 7068 Aluminum Alloy's Youngs Modulus is 73.1, which is a lot lower than low carbon steel thus new deflection is 0.268mm. Although it is still within the operational limit of 0.3mm, potentially it may go past that limit if the stresses were to somehow increase, since the young's modulus has decreased, a slight increase in stress could generate a large deflection. The dynamic analysis shows the most concerning natural frequency of 1256 Hz from the mode 1 is still far away from the natural frequencies of driveshaft or ride frequencies of a F1 car. Therefore, pose no threat to potential resonance.

Additionally, the simulation results were validated through theoretical calculations, proving Abaqus' reliability. Consequently, the iterative methodology has effectively reduced the weight of the shift fork as well as switched to a material with higher yield strength and providing lower manufacturing cost. Further work could include more accurate modelling of the contact gears instead of a solid rigid ring.

Bibliography

[1] L. Qiangwei, "Finite Element Analysis and Vibration Control of Lorry's Shift Mechanism," *IOP Conference Series: Materials Science and Engineering,* vol. 269, 2017.

[2] R. Boyer, G. Welsch and E. W. Collings, Materials Properties Handbook: Titanium Alloys, 1994.

[3] C.Sivakumar, "Natural frequency and deformation analysis of drive shaft for an automobiles," *materialstoday proceededings,* vol. 45, pp. 7031-7042, 2021.

[4] N.Rajeev and PratheekSudi, "Natural Frequency, Ride Frequency and their Influence," *Nandan Rajeev Journal of Engineering Research and Application ,* vol. 9, no. 3, pp. 60-64, 2019.

[5] s. o. e. Univeristy of Warwick, Engineering Data Book 8th edition, 2017.

Appendix

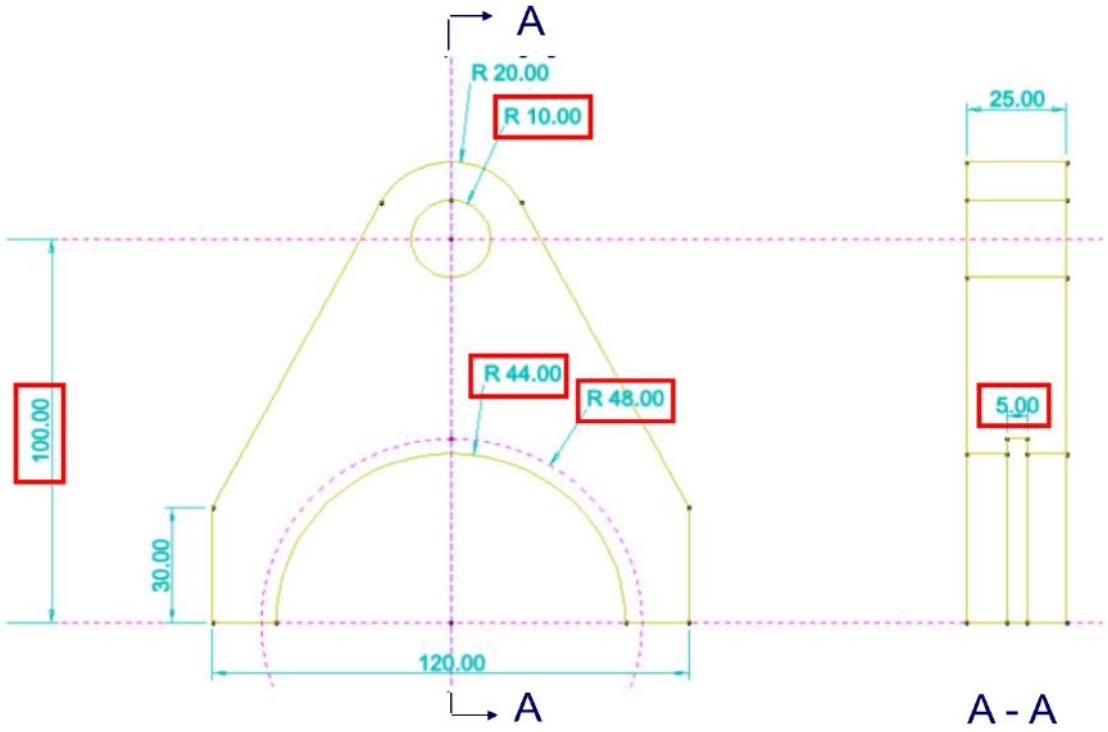

Figure 21: initial design geometry for the shift fork component (unit: mm), with constraints highlighted in red

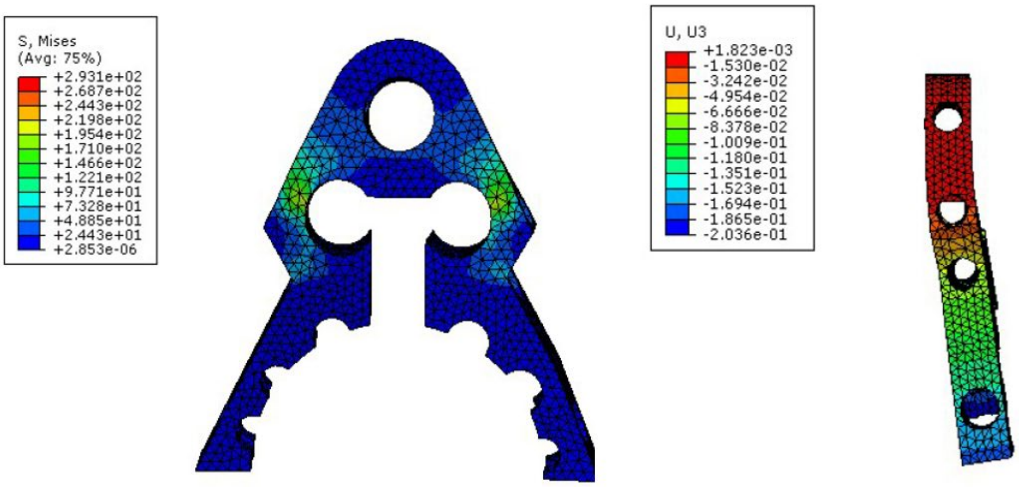

Figure 22: Stress distribution & deflection (U3 direction – axial) of the non-linear analysis on iteration 8

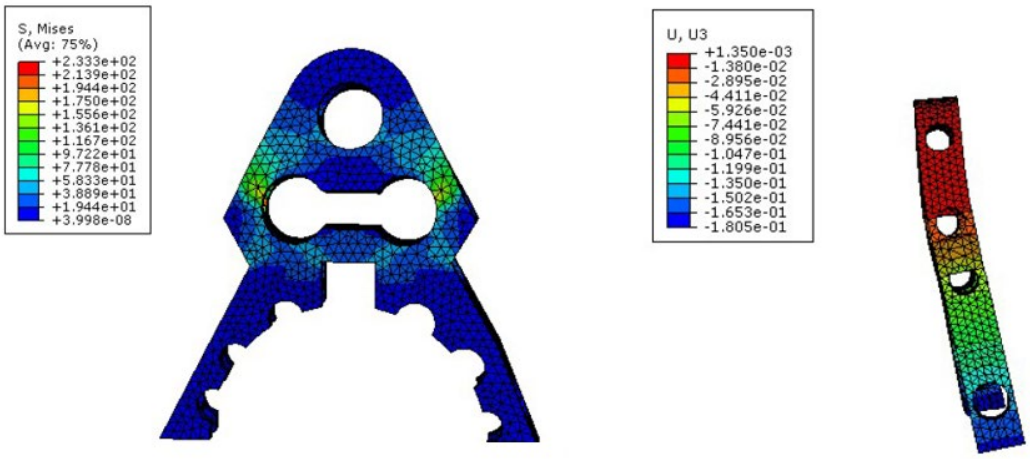

Figure 23: Stress distribution & deflection (U3 direction – axial) of the non-linear analysis on iteration 9

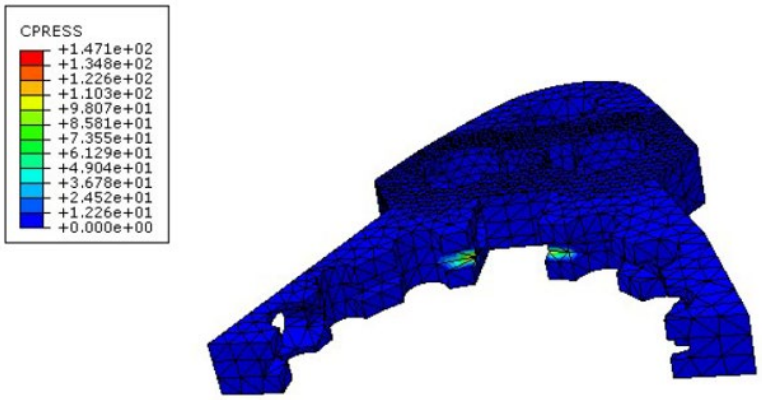

Figure 24: Contact Pressure of the final design (iteration 10) in the non-linear analysis

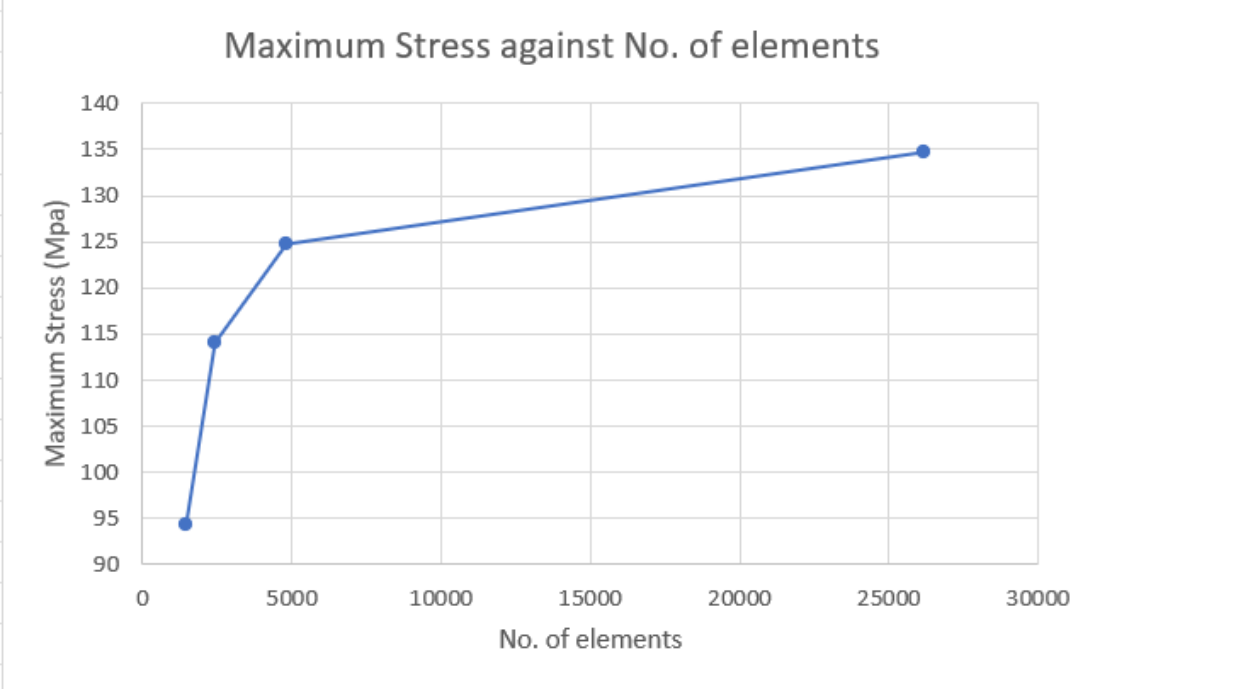

Figure 25: Mesh Convergence graph: Maximum Stress (MPa) plotted against number of elements

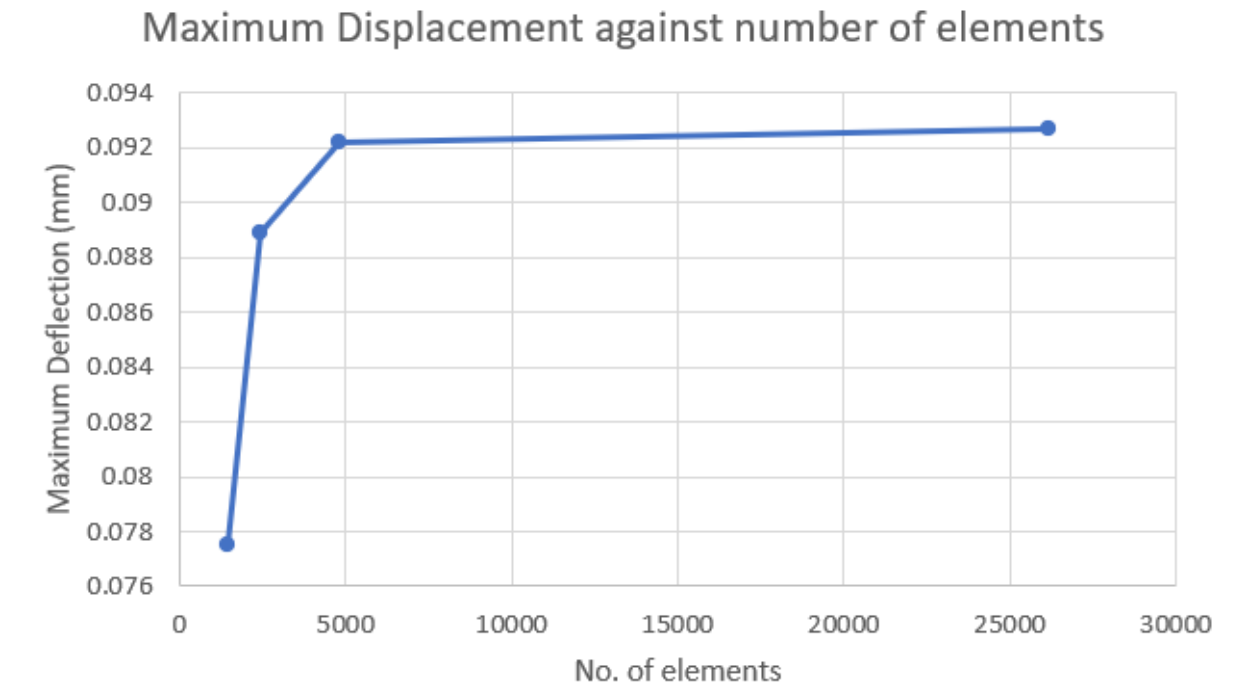

Figure 26: Mesh Convergence graph: Maximum Deflection (mm) plotted against number of elements

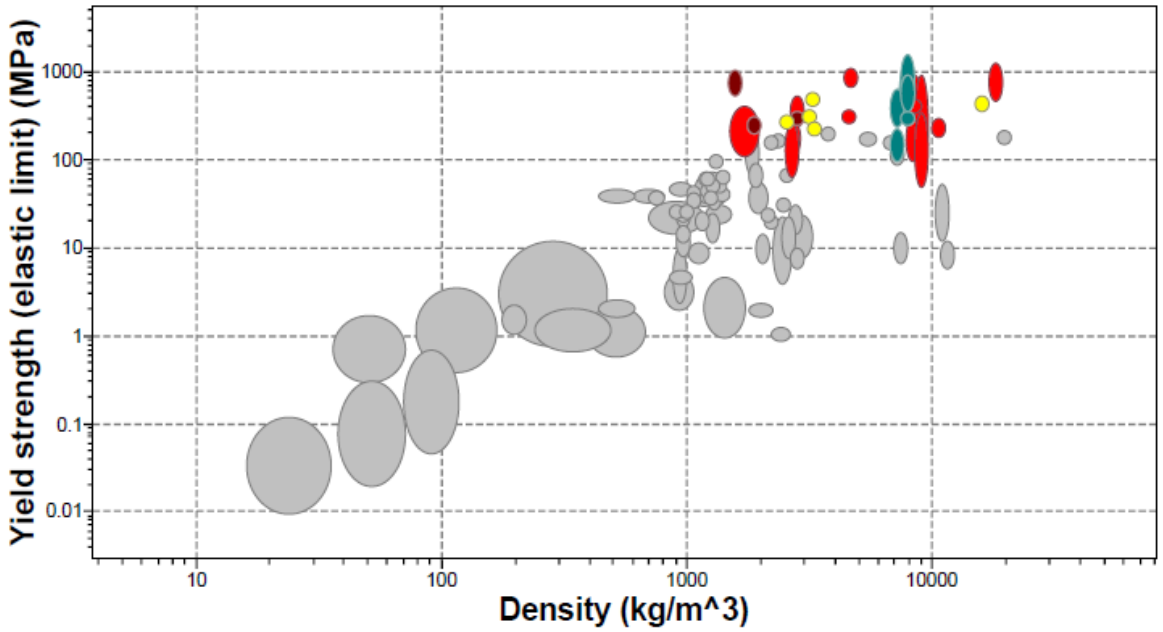

Figure 27: Ansys Granta Edupack material selection graph: Yield strength (MPa) against Density (kg/m^3) (With low cost materials filtered)

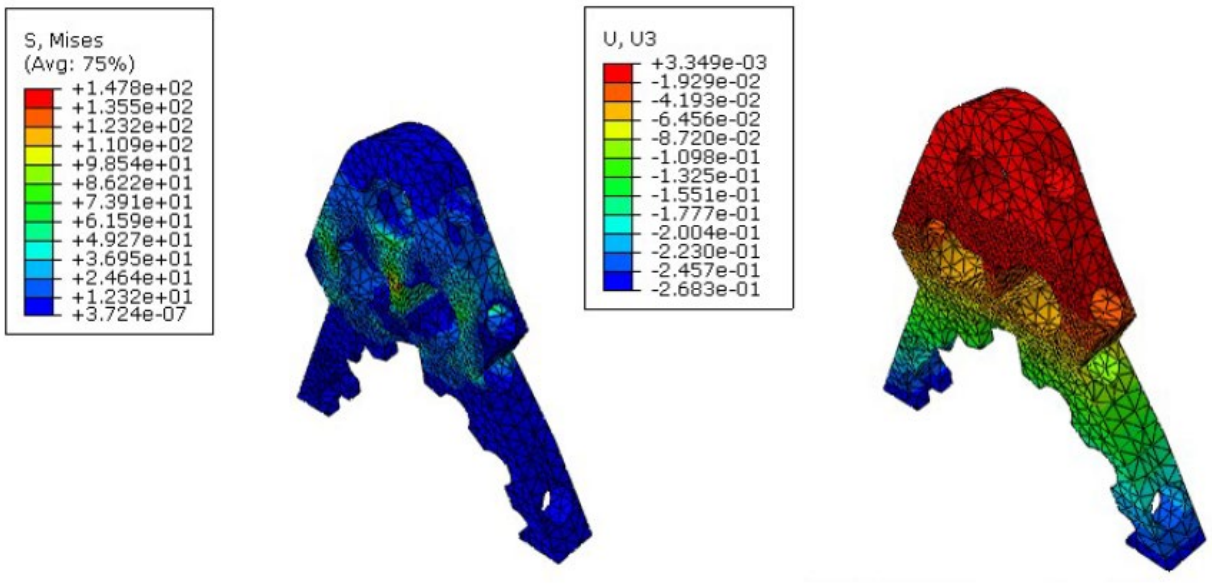

Figure 28: Stress distribution & deflection (U3 direction – axial) of final design made with 7068 Aluminum Alloy